PNAS
www.pnas.org

Supplementary Information for

Mistimed food intake and sleep alters 24 hour time-of-day patterns of the human plasma proteome

Christopher M. Depner[1*], Edward L. Melanson[2,3,4], Andrew W. McHill[1,5,6,7], Kenneth P. Wright Jr.[1,2*]

[1]Sleep and Chronobiology Laboratory, Department of Integrative Physiology, University of Colorado Boulder, Boulder, CO, 80309, USA

[2]Division of Endocrinology, Metabolism, and Diabetes, University of Colorado Anschutz Medical Campus, Aurora, CO, 80045, USA

[3]Division of Geriatric Medicine, University of Colorado Anschutz Medical Campus, Aurora, CO, 80045, USA

[4]Geriatric Research, Education, and Clinical Center, VA Eastern Colorado Health Care System, Denver, CO, 80220, USA

[5]Oregon Institute of Occupational Health Sciences, Oregon Health and Science University, Portland, OR, 97239, USA

[6]Division of Sleep and Circadian Disorders, Department of Medicine, Brigham and Women's Hospital, Boston, MA, 02115

[7]Division of Sleep Medicine, Harvard Medical School, Boston, MA, 02115

[*]Corresponding authors

Email: kenneth.wright@colorado.edu; christopher.depner@colorado.edu

This PDF file includes:

Supplementary text
Figs. S1 to S9
References for SI reference citations

Other supplementary materials for this manuscript include the following:

Dataset S1

Supplementary Information Text

Effect Size Calculations.

Effect sizes using η2G, that account for variance due to individual differences were computed using sum of squares from mixed-effects ANOVA models. Effect sizes were evaluated using Cohen's general cutoffs for η2 of 0.02 as small, 0.13 as medium, and 0.26 as large. Measures of η2G are generally smaller than the commonly reported partial eta-squared (η2p). The use of η2G allows comparison of effect size across studies with similar target populations regardless if factors of interest were studied using between or within-subject designs (1, 2).

Detailed Parameters for Detection of Differential Rhythmicity (DODR v0.99.2) Analysis.

A data matrix for study day 2 (circadian alignment) and study day 4 (circadian misalignment) each containing the average protein levels for all subjects at one time-point using difference from the mean data was entered in R (v3.3.1) for analysis. "Period" was set to 24h, the "robust" method was used which combines the "robustDODR" and "robustHarm-ScaleTest", normalization was set to "FALSE". We used the "meta.p.value" output which contains the lowest *P*-value from the "robustDODR" and "robustHarm-ScaleTest" tests and is corrected for multiple comparisons using a beta-distribution approach.

Detailed Parameters for Extraction of Differential Gene Expression (EDGE v2.4.2) Analysis.

A data matrix containing difference from the mean data for each individual subject at all time-points on study day 2 (circadian alignment) and study day 4 (circadian misalignment) was entered in R (v3.3.1) for analysis. The function "build_study" was used to build the full (differential

expression) and null (no differential expression) models with the sampling method set to "timecourse". The full and null models were then fit to the data using the "fit_models" function with "stat.type" set to "odp". Then, to test if the full model fits the data better than the null model, we implemented the optimal discovery procedure (ODP) using the "odp" function with "bs.its" (bootstrap iterations) set to 50 and "n.mods" (number of clusters in k-means algorithm) set to 50 as recommended by Storey et al (3). We used the "qvalues" (false discovery rate corrected) output to identify proteins where the full model fits the data better than the null model (significant differential expression between study days).

Detailed Parameters for Identifying Significant Clusters for Proteins with Significantly Different 24h Time-of-day Patterns.

A data matrix containing mean z-scored data (using grand mean and standard deviations) for each time-point on each study day for the 76 proteins identified with significantly different 24h time-of-day patterns was entered in R (v3.3.1) for analysis. The Pvclust package (v2.0-0) was used for cluster analyses. Within pvclust, we used the "pvclust" function, with "method.hclust" set to "ward.d", "method.dist" set to "uncentered", and "nboot" set to 10,000. To identify statistically significant clusters, we used the "pvrect" function with "alpha" set to "0.95".

Detailed Parameters for Linear Mixed Models.

Linear mixed models were analyzed using the lme4 package (v1.1-12) in R (v3.3.1). Within lme4, we used the "lmer" function, with "REML" set to "FALSE". *P*-values for the models assessing the associations of fibroblast growth factor 19 and the creatine kinase isoforms with energy expenditure were determined using the "cftest" function within the "multcomp" package (v1.4-6).

Detailed Parameters for Mixed Effects Models with Cubic Time-Components.

Linear mixed effect models with a cubic term were analyzed using the nlme package (v3.1-131) in R (v3.3.1). Within nlme, we used the "lme" function and the model for each protein was fit with a linear, quadratic and cubic term ($y = t + t^2 + t^3$). The significance for the cubic term was determined using an ANOVA model with marginal sum of squares.

Detailed Parameters for MetaCycle (v1.1.0) Analyses.

A data matrix containing difference from the mean data for each individual subject at all time-points on study day 2 (circadian alignment) and study day 4 (circadian misalignment) was entered in R (v3.3.1) for analysis. To detect proteins with 24h time-of-day patterns, the function "meta3d" was used with "cycMethodOne" set to "ARS", "JTK", and "LS" for each of the Arser, JTK, and Lomb-Scargle analyses, respectively. The time unit for all metacycle analyses was set to "hour" and "dayZeroBased" was set to "FALSE". To estimate the phase of proteins with a detected 24h time-of-day pattern for both circadian alignment and misalignment, the function "meta2d" was used with "cycMethod" set to "JTK" and "LS", "adjustPhase" set to "predictedPer", and "weightedPerPha" set to "TRUE". Data from the circadian aligned (study day 2) and misaligned (study day 4) days were analyzed separately for phase analyses.

Detailed Parameters for Significance Analysis of Microarray (SAM) Analyses.

A data matrix containing average protein abundance data for each individual subject on study day 2 (circadian alignment) and study day 4 (circadian misalignment) was entered in R (v3.3.1) for analysis using the package SAMR v2.0. To identify proteins with significantly altered average 24h levels during circadian misalignment versus alignment, the function "SAM" was used with "resp.type" set to "Two class paired" and "nperms" set to "1000".

Supporting Results and Discussion

Peptide YY (PYY). In the larger sample from this study, we reported the appetitive hormone PYY predominantly followed the behavioral sleep-wake/fasting-food intake cycle (4). Here, as assessed in the proteomics platform, PYY had a significantly different 24h time-of-day pattern when circadian misaligned versus aligned with peak levels during scheduled wakefulness for both circadian alignment and misalignment (Fig. S3B). These current findings are similar to the findings from the larger sample from this study (4).

Glucose and Insulin. In response to food intake in healthy individuals, pancreatic beta cells secrete insulin, stimulating glucose uptake by insulin sensitive tissues. Based on our proteomics analyses, 24-h average insulin concentration (circadian misalignment 75.7±1.7 RFU; circadian alignment 71.9±2.1 RFU) was ~5% higher ($P < 0.05$) during circadian misalignment versus alignment with a small effect size ($\eta^2_G = 0.09$) for study day (Fig. S5F). Additionally, insulin trapezoidal AUC (circadian misalignment 77.1±1.5 RFU x hour; circadian alignment 73.1±1.5 RFU x hour) during scheduled wakefulness was ~5% higher ($P < 0.05$) during circadian misalignment versus alignment (Fig. S5F). Higher insulin concentration is suggestive of reduced insulin sensitivity or reduced insulin clearance during circadian misalignment, consistent with prior findings (5). We also analyzed plasma glucose at the same time-points used for the proteomic analyses and found lower ($P < 0.05$) glucose concentration during sleep regardless of circadian timing (Fig. S5E). Given the 4h frequency of sampling for these 24h insulin and glucose analyses, we may have missed peaks associated with food intake and thus future trials with more frequent sampling are needed.

Insulin Like Growth Factor-1 (IGF-1) and IGF-Binding Proteins (IGFBP). Classically, IGF-1 is considered a growth factor but findings also implicate IGF-1 in blood glucose regulation (6). Here, IGF-1 did not change during circadian misalignment versus alignment (Fig. S2A), but we

found that four out of seven IGFBPs analyzed were altered during circadian misalignment versus alignment (Fig. S2B-H). IGFBP-1 was elevated ~88% ($P < 0.01$) with a large effect size for study day ($\eta^2_G = 0.46$), and had a significantly different 24h time-of-day pattern when circadian misaligned versus aligned (Fig. S2B). Our findings showing a change in the 24h time-of-day pattern in IGFBP-1 with peak levels occurring near the end of the daytime sleep opportunity during circadian misalignment are similar to previous findings where sleep and food intake were delayed by 8h (7). Previously, IGFBP-1 was found to reduce plasma glucose concentrations (8), and IGFBP-1 is reportedly lower in obese individuals (9). Thus, elevated IGFBP-1 during circadian misalignment could represent an unsuccessful physiological response to maintain blood glucose levels in the healthy individuals studied here. Further studies are needed to determine the impact of circadian misalignment on IGFBP-1 in at risk individuals including shift-workers and those with obesity and type 2 diabetes. Our findings show IGFBP-2 was elevated ~20% ($P < 0.05$) with a large effect size for study day ($\eta^2_G = 0.53$), and had a significantly different 24h time-of-day pattern when circadian misaligned versus aligned (Fig. S2C). Peak levels for IGFBP-2 occurred during scheduled wakefulness for circadian alignment and misalignment showing the behavioral cycle regulates IGFBP-2. The potential impact of IGFBP-2 on glucose metabolism is unclear. In one study, transgenic mice overexpressing IGFBP-2 had impaired glucose clearance (10), whereas in a different study, mice overexpressing human IGFBP-2 had improved insulin sensitivity (11). Obese humans have lower IGFBP-2 concentrations (12) and IGFBP-2 independently predicts insulin sensitivity (13). Further studies are required to better define the role of IGFBP-2 in glucose metabolism during circadian misalignment and alignment and determine if such effects are mediated through or independent of IGF-1. Abundance of IGFBP-3 showed no statistically significant differences between circadian misalignment and alignment (Fig. S2D). IGFBP-3 is the most abundant IGFBP and findings show IGFBP-3 positively correlates with glycated hemoglobin, a long-term marker of blood glucose concentration, and IGFBP-3 is elevated in individuals with

type 2 diabetes (6). IGFBP-4 had a significantly different 24h time-of-day pattern when circadian misaligned versus aligned (Fig. S2E). Visually, IGFBP-4 does not appear to have different 24h time-of-day patterns during circadian misalignment versus alignment. These findings are one example where higher sampling frequency and sampling over multiple 24h cycles may yield different findings. Given the nature of large-scale omics analyses, some false positives are expected even when correcting for multiple comparisons. IGFBP-4 binds and inhibits IGF-1 and was recently reported to be lower in patients with type 2 diabetes (14). However, IGFBP-4 knockout mice had improved responses to glucose challenge versus wild type mice (15). Thus, to determine if IGFBP-4 directly regulates glucose metabolism or impacts glucose metabolism by modulating IGF-1 requires further research under conditions of both circadian alignment and misalignment. IGFBP-5 and -6 showed no statistically significant differences between circadian misalignment and alignment (Fig. S2F,G). IGFBP-5 is reportedly lower in individuals with diabetes (16), and IGFBP-5 knockout mice have reduced insulin sensitivity that is exacerbated by diet-induced obesity (17). No known findings directly implicate IGFBP-6 in regulating glucose metabolism. IGFBP-7 was reduced ~9% ($P < 0.01$) when circadian misaligned versus aligned with a large effect size for study day ($\eta^2_G = 0.30$; Fig. S2H). IGFBP-7 binds insulin and is elevated in subjects with metabolic syndrome and insulin resistance (18, 19). Our finding of reduced IGFBP-7 during circadian misalignment in healthy subjects suggests IGFBP-7 does not contribute to glucose dysregulation during circadian misalignment. Reduced IGFBP-7 during circadian misalignment in healthy individuals may represent an unsuccessful physiological response to maintain normal glucose levels and further studies in shift-workers, obese, and type 2 diabetic subjects are needed to determine any impact of circadian misalignment on IGFBP-7 in at risk populations. While we identified several proteins involved in the IGF-1 axis were altered during circadian misalignment in healthy individuals, circadian misalignment did not alter abundance of IGF-1, and the observed changes in IGFBP-1 and -7 would be expected to improve not impair glucose metabolism. Overall, given the established role of the IGF axis in regulating glucose metabolism (6), further studies in

shift-workers, obese, and type 2 diabetic individuals are needed to determine how circadian misalignment impacts the IGF axis in at risk populations.

Lipocalin-2. Abundance of lipocalin-2, an adipokine implicated in insulin sensitivity (20), was similar during circadian misalignment versus alignment (Fig. S6A) and thus may not be a contributor to metabolic dysregulation during circadian misalignment.

Kallikrein-7. Kallikrein-7, a protease that reportedly cleaves human insulin (21), was reduced ~13% ($P < 0.01$) with a large effect size for study day ($\eta^2_G = 0.26$), and had a significantly different 24h time-of-day pattern when circadian misaligned versus aligned (Fig. S6B). Thus, altered levels of kallikrein-7 may contribute to elevated insulin concentration during circadian misalignment.

Adiponectin. Adiponectin is a hormone released by adipose cells that has established insulin sensitizing effects by activating 5'-AMP-activated protein kinase (22). Individuals with obesity and type 2 diabetes have lower circulating adiponectin concentration (23). Given the well-established insulin sensitizing effect of adiponectin (22) and findings showing early morning shiftwork reduces adiponectin (24), we hypothesized that circadian misalignment would reduce adiponectin compared to circadian alignment in our protocol. Our proteomics analyses show ~9% reduced ($P < 0.05$) plasma adiponectin concentration when circadian misaligned versus aligned with a small effect size for study day ($\eta^2_G = 0.12$; Fig. S6C). Our findings suggest reduced adiponectin during circadian misalignment may contribute to the elevated glucose and insulin responses to the breakfast test meal when circadian misaligned versus aligned. However, given the small effect size, our findings require validation in a study with larger sample sizes.

PI3K. PI3K is a kinase involved in cell signaling pathways of multiple growth factors including insulin. Our findings show average PI3K abundance was elevated ~6% ($P < 0.05$) when circadian misaligned versus aligned with a medium effect size for study day ($\eta^2_G = 0.21$; Fig. S6D). Elevated PI3K levels could affect the insulin signaling cascade, however, we cannot determine the phosphorylation status of PI3K or its downstream targets in the current study. Future studies need to specifically investigate the impact of elevated PI3K on glucose metabolism during circadian misalignment including tissue specific analyses to determine the source of elevated PI3K. Previous findings in mice show peak expression of the regulatory PI3K subunit, *Pik3r1*, occurs at different times in different organs (25).

Erythropoietin (EPO). EPO is a hormone that controls erythropoiesis (26). Findings from nocturnal rodent studies suggest high glucose levels stimulate EPO production and elevated EPO has been reported to improve glucose regulation (27) and be protective against diabetic nephropathy, at least in its early stages (28). Our findings show average EPO abundance was elevated ~8% ($P < 0.01$) when circadian misaligned versus aligned with a medium effect size for study day ($\eta^2_G = 0.19$; Fig. S6E), potentially in response to elevated plasma glucose (Fig. 5A), and thus requiring further investigation in humans.

Hepcidin (LEAP-1). Previous findings show body iron overload is common in type 2 diabetic patients and in individuals with reduced glucose tolerance (29). Furthermore, iron overload is known to contribute to development and progression of type 2 diabetes by inducing oxidative stress in hepatocytes and pancreatic beta cells (30, 31). Findings from animal and cell culture studies indicate hepcidin (LEAP-1), the primary hormone controlling whole-body iron homeostasis, is regulated by insulin (32) and glucagon (33). Here, LEAP-1 had a significantly different 24h time-of-day pattern when circadian misaligned versus aligned, with peak levels occurring during

scheduled wakefulness for both circadian alignment and misalignment (Fig. S6G). This observed pattern of plasma LEAP-1 levels is similar to plasma glucagon and supports prior findings showing glucagon regulates LEAP-1 expression. Furthermore, our findings show LEAP-1 is regulated by the behavioral cycle and thus will become misaligned with the endogenous master circadian suprachiasmatic nucleus clock during circadian misalignment. These findings warrant further investigation into the impact of circadian misalignment on LEAP-1 in at risk populations including shift-workers, pre-diabetics, overweight/obese, and older age and potential roles in metabolic dysregulation.

Diseases Associated with Altered Proteins when Circadian Misaligned Versus Aligned. We conducted gene ontology (GO) disease association analyses using the 62 proteins with altered average 24h levels and the 76 proteins with significantly different 24h time-of-day patterns when circadian misaligned versus aligned. Eleven proteins with significantly different 24h time-of-day patterns also had altered average 24h levels when circadian misaligned versus aligned, thus 127 total proteins were included in these analyses. Diseases associated with these proteins include coronary artery disease, kidney failure, and several types of cancer, consistent with higher risk of such diseases reported in epidemiological studies of shift-work (Fig. S7) (34-36).

Modeling 24h Time-of-Day Patterns. As recently demonstrated by Wu et al., (37) using both computer generated and previously collected yeast and mouse datasets, selecting the best algorithm to detect rhythmicity in high-dimensional datasets is not straightforward and generally no single algorithm will optimally fit all biological rhythms. Numerous factors such as the underlying shape of the rhythm, noise distribution, missing data, frequency of sample collection, and experimental design can impact which algorithm may optimally detect a biological rhythm. Here, since our data does not include two or more full 24h cycles, we chose to use mixed-effects cubic modeling in conjunction with MetaCycle (37) that was specifically designed to analyze high-dimensional time-

series datasets. As may be expected, the outcomes of these different algorithms had little overlap. In general, mixed-effects cubic models were more likely to detect significant 24h time-of-day patterns in some proteins with bi-modal peaks whereas MetaCycle generally did not detect significant 24h time-of-day patterns in proteins with bi-modal peaks (Fig. S8A and S9B). Similar to our mixed-effects cubic models, findings from human transcriptomics studies (38, 39) that fit a sinusoidal function to transcriptomics data and used an R^2 cut-off to define 24h time-of-day patterns also show some transcripts with bi-modal peaks that fit their criteria for 24h time-of-day patterns. Regardless of the algorithm used, further studies are needed to confirm these 24h time-of-day patterns and define the amplitude and phase of proteins of interest using other protocols such as the constant routine.

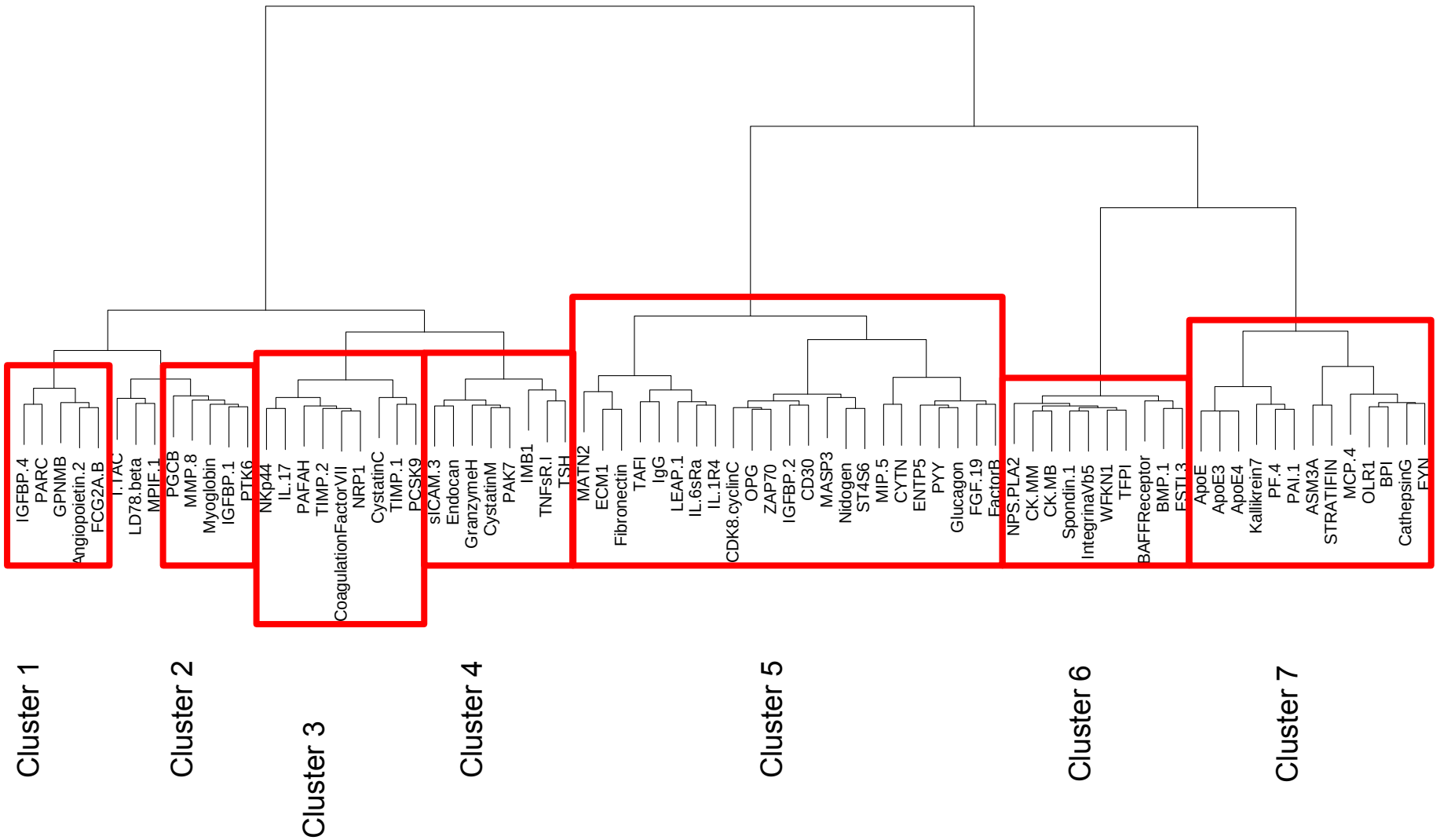

Figure S1. Bootstraped heirarchical cluster dendrogram for plasma proteins with significantly different 24h time-of-day patterns during circadian misalignment versus alignment. All 76 proteins identified with significantly different 24h time-of-day patterns when circadian misaligned versus aligned by the EDGE and DODR analyses were included in cluster analyses. Red boxes represent statistically significant clusters at the $P < 0.05$ level. Cluster numbers coorespond to cluster numbers presented in Figure 3.

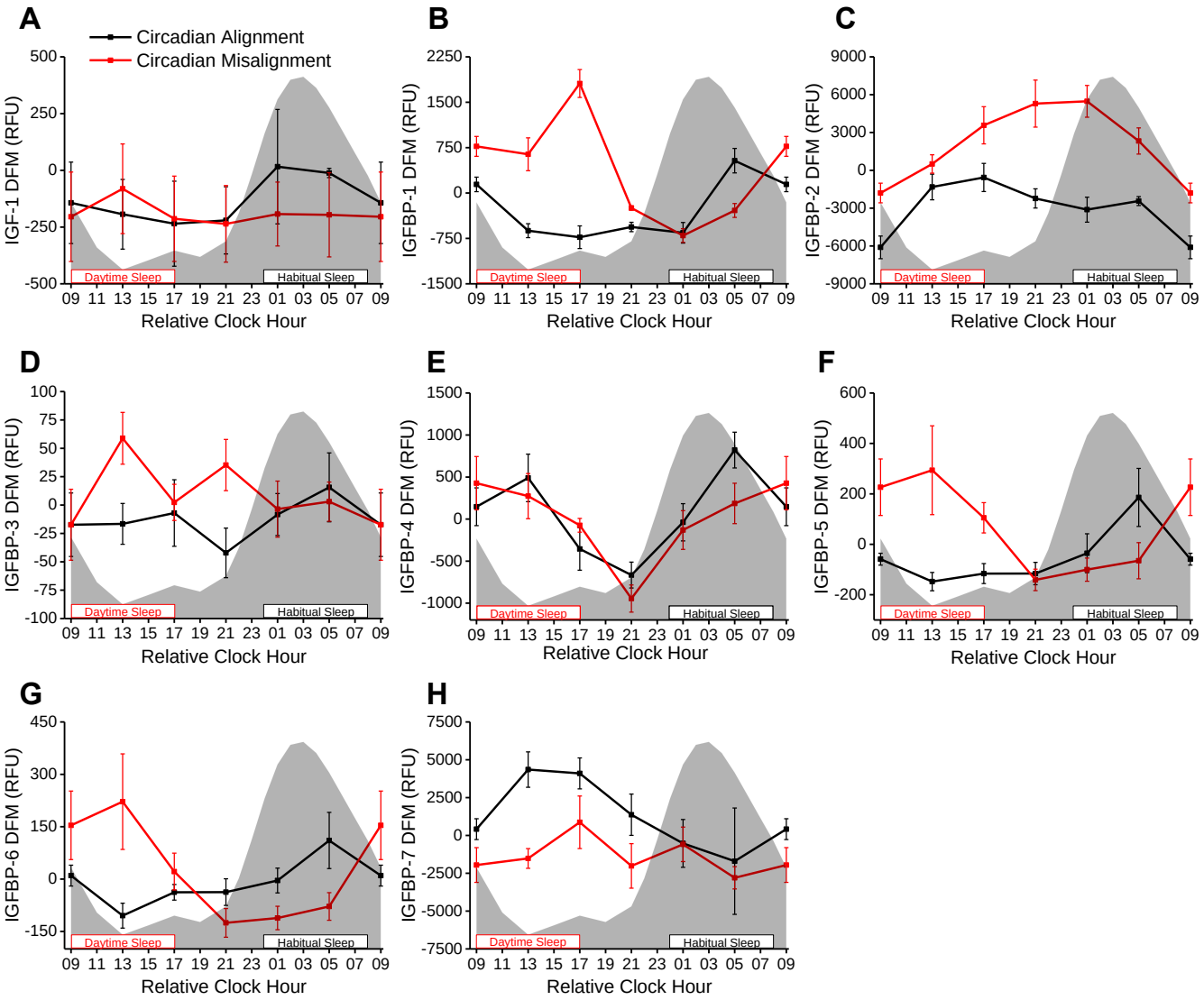

Figure S2. Proteins in the insulin like growth factor axis analyzed by the proteomics platform (n = 6). (A) IGF-1; (B) IGFBP-1 (study day SAM FDR = 0.03); (C) IGFBP-2 (study day SAM FDR = 0.05); (D) IGFBP-3; (E) IGFBP-4; (F) IGFBP-5; (G) IGFBP-6; (H) IGFBP-7 (study day SAM FDR < 0.01). Gray shading represents the average fitted melatonin values across circadian alignment and misalignment conditions. Black and red outlined rectangles represent scheduled sleep opportunities during circadian alignment (habitual sleep) and circadian misalignment (daytime sleep), respectively. IGFBP-1 (EDGE; FDR = 0.026), IGFBP-2 (DODR; P = 0.016), and IGFBP-4 (DODR; P = 0.03) have significantly different 24h time-of-day patterns when circadian misaligned versus aligned. All data are mean ± SEM. Data for relative clock hour 09 is re-plotted for visual purposes only and was not used for any analyses. DFM, difference from mean; RFU, relative flouresence units; IGF, insulin like growth factor; IGFBP, insulin like growth factor binding protein.

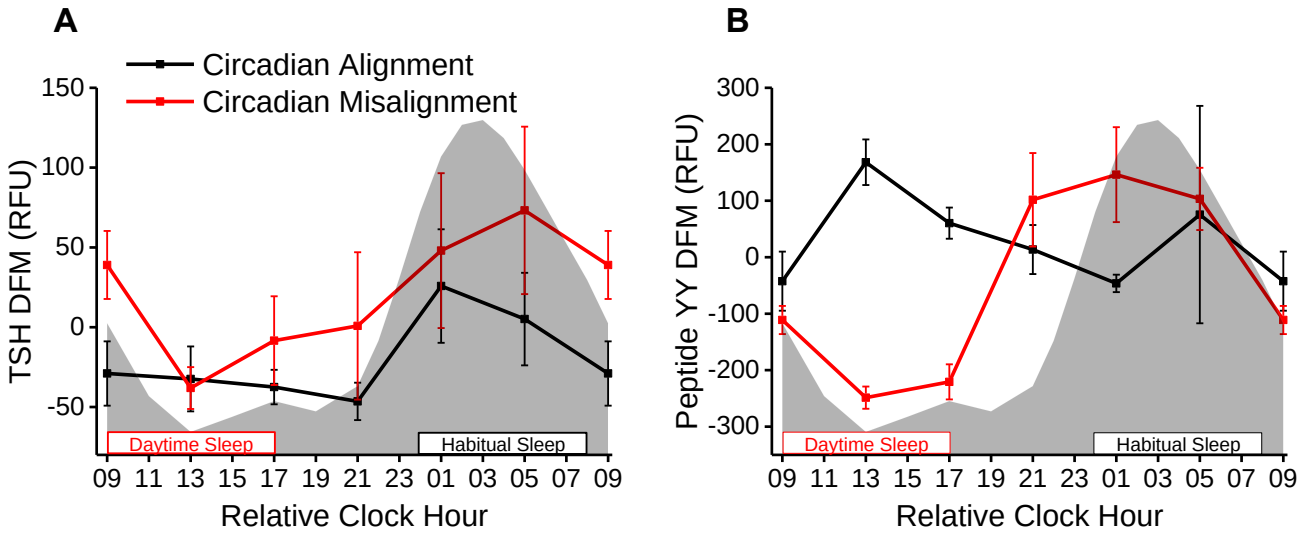

Figure S3. Protein hormones with known circadian and behavioral cycle modulation (n = 6). (A) TSH (B) Peptide-YY. Gray shading and black and red boxes and lines as in Figure S2. TSH (DODR; P = 0.021) and peptide-YY (EDGE; FDR = 0.002) have significantly different 24h time-of-day patterns when circadian misaligned versus aligned. All data are mean ± SEM. Data for relative clock hour 09 is re-plotted for visual purposes only and was not used for any analyses. DFM, difference from mean; RFU, relative flouresence units; TSH, thyroid stimulating hormone.

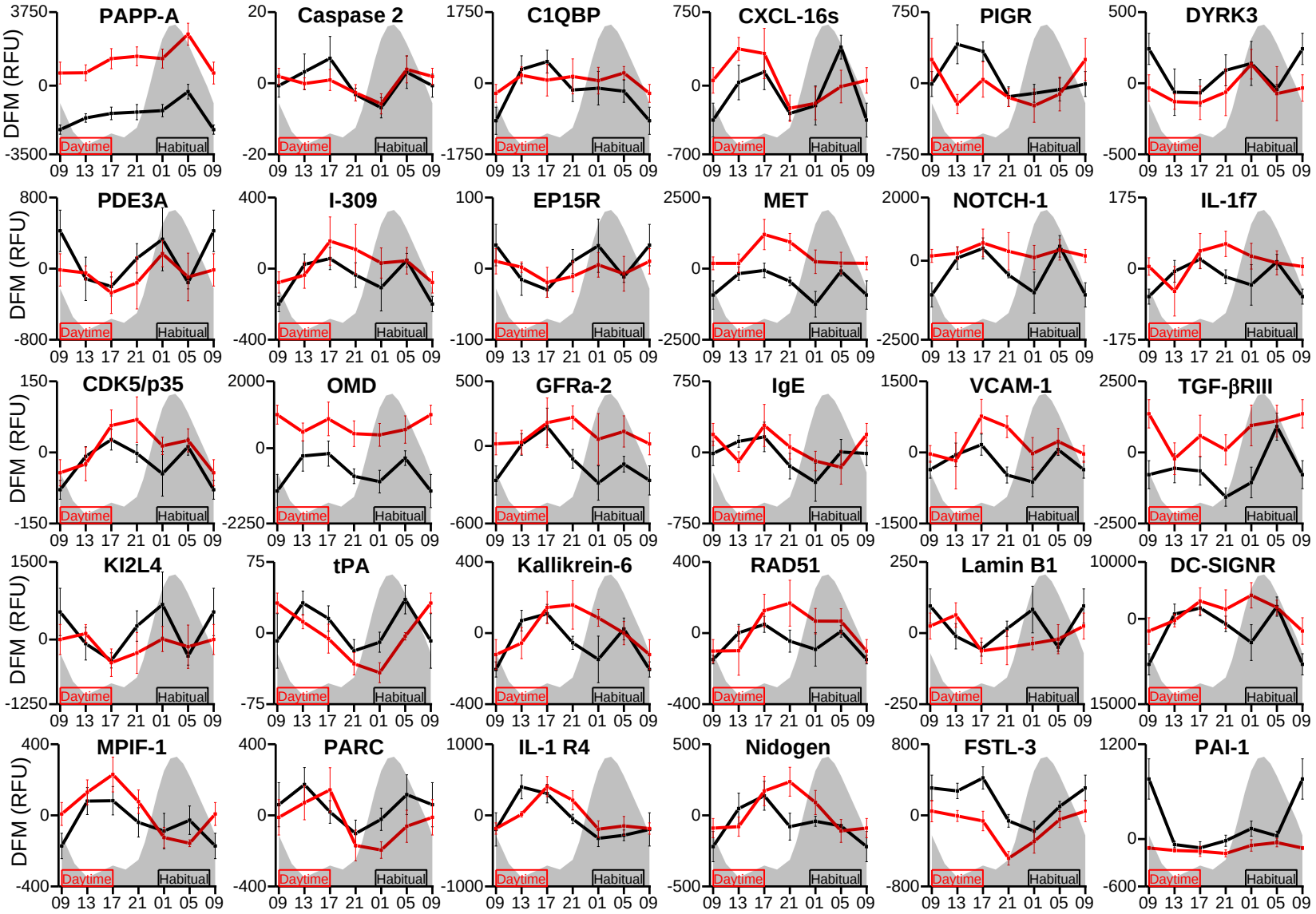

Figure S4. Plasma proteins with circadian regulated 24h time-of-day patterns as identified by MetaCycle and mixed-effects cubic models. All 30 proteins identified with circadian regulated time-of-day patterns are represented. Gray shading and black and red boxes and lines as in Figure S2. Data

are mean ± SEM. DFM was calculated for each subject individually using the grand mean of all samples within each individual subject. Data for relative clock hour 09 as in Figure 3. DFM, difference from mean; RFU, relative fluorescence units; PAPP-A, pappalysin-1; C1QBP, complement component 1 Q subcomponent-binding protein mitochondrial; CXCL-16 Soluble, C-X-C motif chemokine 16; PIGR, polymeric immunoglobulin receptor; DYRK3, dual specificity tyrosine-phosphorylation-regulated kinase 3; PDE3A, cGMP-inhibited 3',5'-cyclic phosphodiesterase A; I-309, C-C motif chemokine 1; EP15R, epidermal growth factor receptor substrate 15-like 1; MET, hepatocyte growth factor receptor; NOTCH1, neurogenic locus notch homolog protein 1; IL-1f7, interleukin-37; CDk5/p35, cyclin-dependent kinase 5:Cyclin-dependent kinase 5 activator 1 complex; OMD, osteomodulin; GFRa-2, GDNF family receptor alpha-2; IgE, immunoglobulin E; VCAM-1, vascular cell adhesion protein 1; TGFβRIII, transforming growth factor beta receptor type 3; KI2L4, killer cell immunoglobulin-like receptor 2DL4; tPA, tissue-type plasminogen activator; RAD51, DNA repair protein RAD51 homolog 1; DC-SIGNR, C-type lectin domain family 4 member M; MPIF-1, C-C motif chemokine 23; PARC, C-C motif chemokine 18; IL-1 R4, interleukin-1 receptor-like 1; FSTL-3, follistatin-related protein 3; PAI-1, plasminogen activator inhibitor 1.

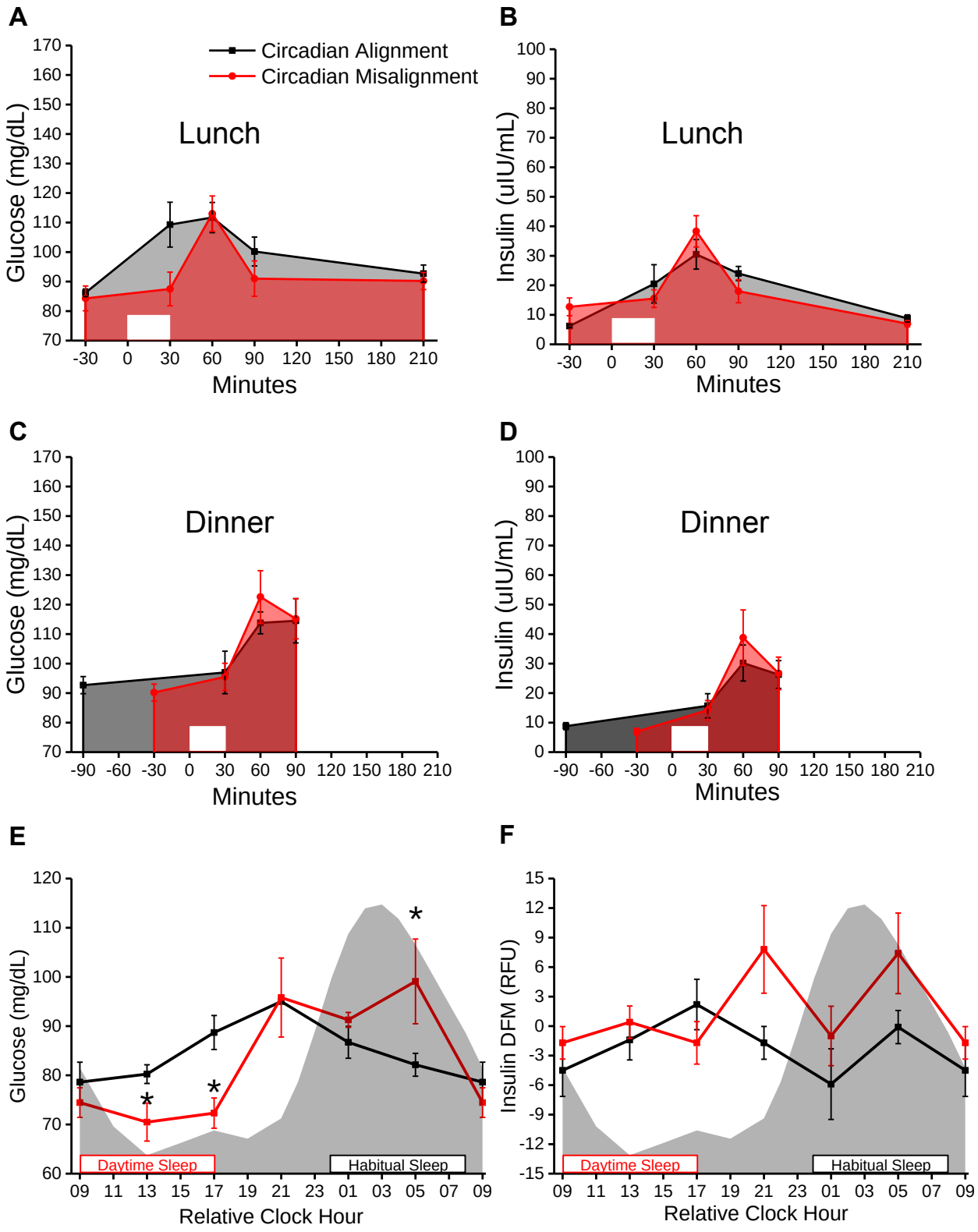

Figure S5. Glucose and insulin responses (n = 6). (A) Postprandial plasma glucose; and (B) postprandial plasma insulin following fixed lunch meals. (C) Postprandial plasma glucose; and (D) postprandial plasma insulin following fixed dinner meals. (E) Plasma glucose concentrations at the same time-points used for proteomics analyses (time $P = 0.0009$, study day*time $P = 0.004$; mixed-model ANOVA). (F) Plasma insulin

measured from the proteomics platform (study day $P = 0.02$; mixed-model ANOVA). White rectangles represent the time (30min) allocated to ingest the meals. For the dinner meals, baseline glucose and insulin were analyzed at 90m prior to ingestion of the dinner meal during circadian alignment and 30m prior to ingestion of the dinner meal during circadian misalignment. Gray shading and black and red boxes and lines as in Figure S2. *$P < 0.05$ (one-tailed t-test) versus circadian alignment at same time-point. Data are mean ± SEM. DFM was calculated for each subject individually using the grand mean of all samples within each individual subject. Data for relative clock hour 09 is re-plotted for visual purposes only and was not used for any analyses. DFM, difference from mean; RFU, relative florescence units.

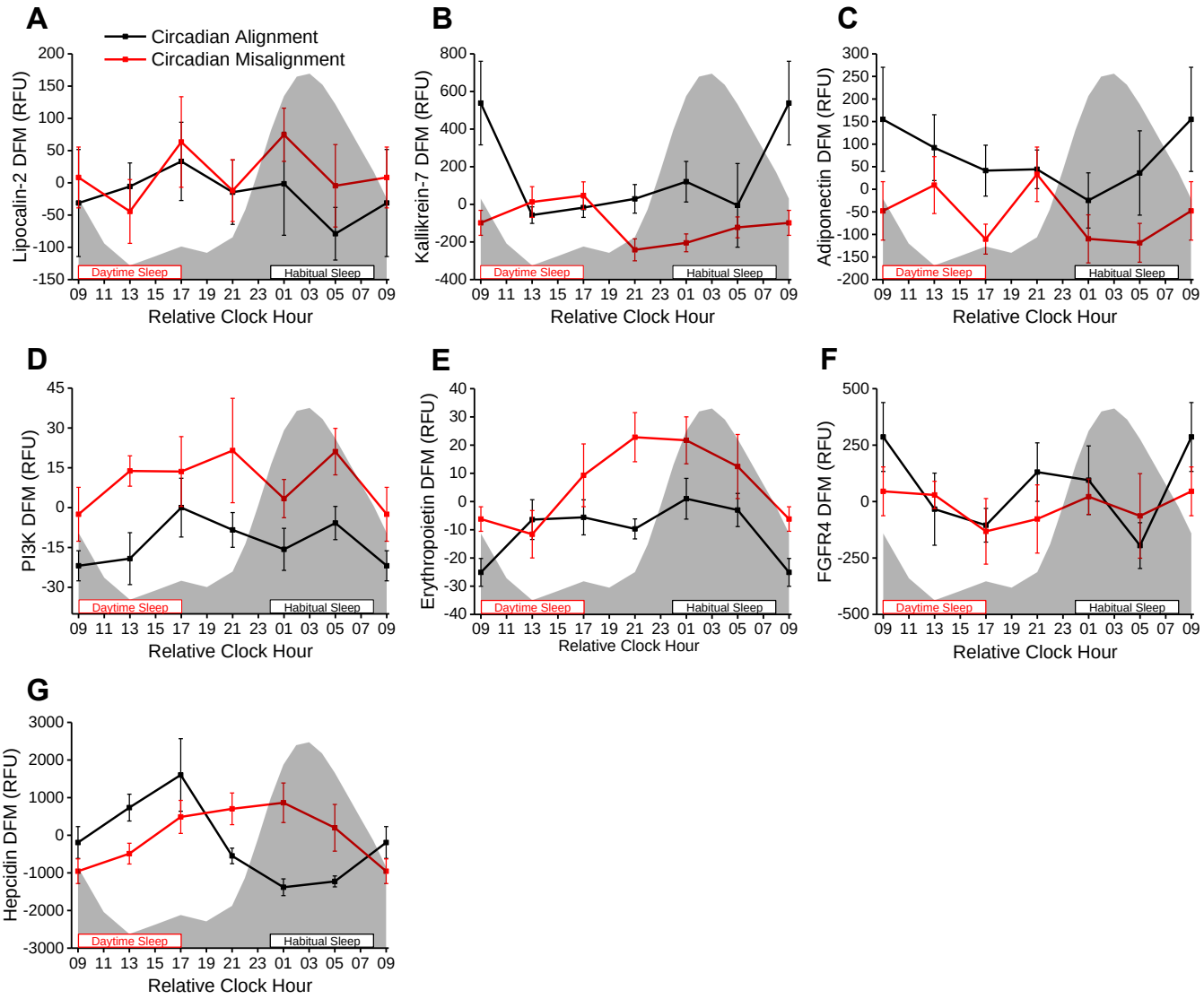

Figure S6. Plasma proteins with known links to metabolic dysregulation analyzed by the proteomics platform (n = 6). (A) lipocalin-2; (B) kallikrein-7 ($P < 0.01$ mixed-model ANOVA); (C) adiponectin ($P < 0.05$ mixed-model ANOVA); (D) PI3K ($P < 0.05$ mixed-model ANOVA); (E) erythropoietin ($P < 0.01$ mixed-model ANOVA); (F) FGFR4; (G) hepcidin. Gray shading and black and red boxes and lines as in Figure S2. Kallikrein-7 (EDGE; FDR = 0.045) and hepcidin (EDGE; FDR = 0.002) have significantly different 24h time-of-day patterns when circadian misaligned versus aligned. All data are mean ± SEM. Data for relative clock hour 09 is re-plotted for visual purposes only and was not used for any analyses. DFM, difference from mean; RFU, relative flouresence units; PI3K, phosphatidylinositol 4,5-bisphosphate 3-kinase catalytic subunit alpha isoform; FGFR4, fibroblast growth factor receptor-4.

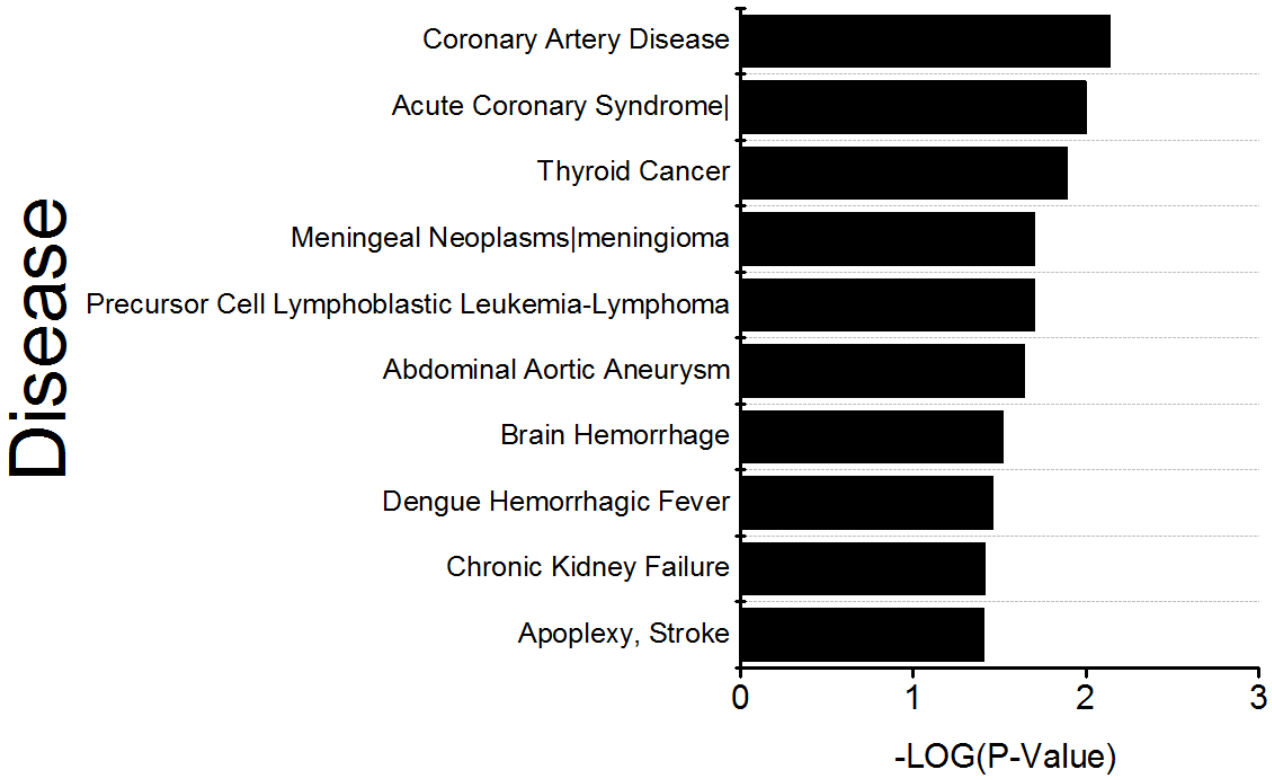

Figure S7. Diseases associated with altered proteins when circadian misaligned versus aligned (n = 6). Proteins used for analyses include all those with altered 24h average levels (2-way ANOVA) and/or different 24h time-of-day patterns when circadian misaligned versus aligned (EDGE and DODR), consisting of 214 total proteins. Diseases were nominally statistically significant at the $P < 0.05$ level.

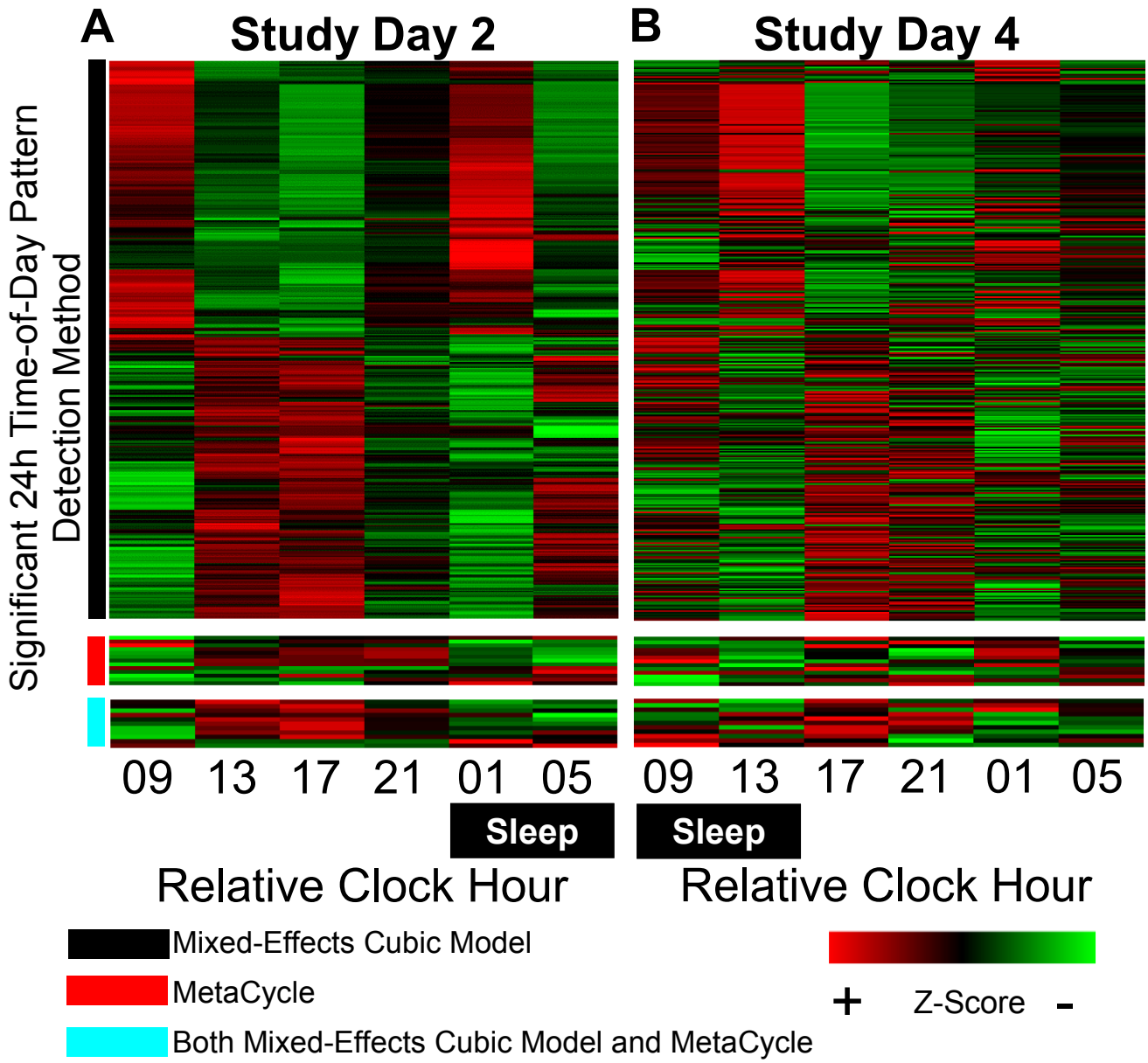

Figure S8. Heat-maps representing proteins with a significant 24h time-of-day pattern during circadian alignment (study day 2). Average z-score profiles are represented for circadian alignment (A) and circadian misalignment (B). On the y axes, the black box indicates proteins with significant 24h time-of-day patterns detected by mixed-effects cubic models, the red box indicates proteins with significant 24h time-of-day patterns detected by MetaCycle, and the cyan box indicates proteins with significant 24h time-of-day patterns detected by both the mixed-effects cubic models and MetaCycle. Black boxes on the x axes represent the timing of scheduled sleep opportunities.

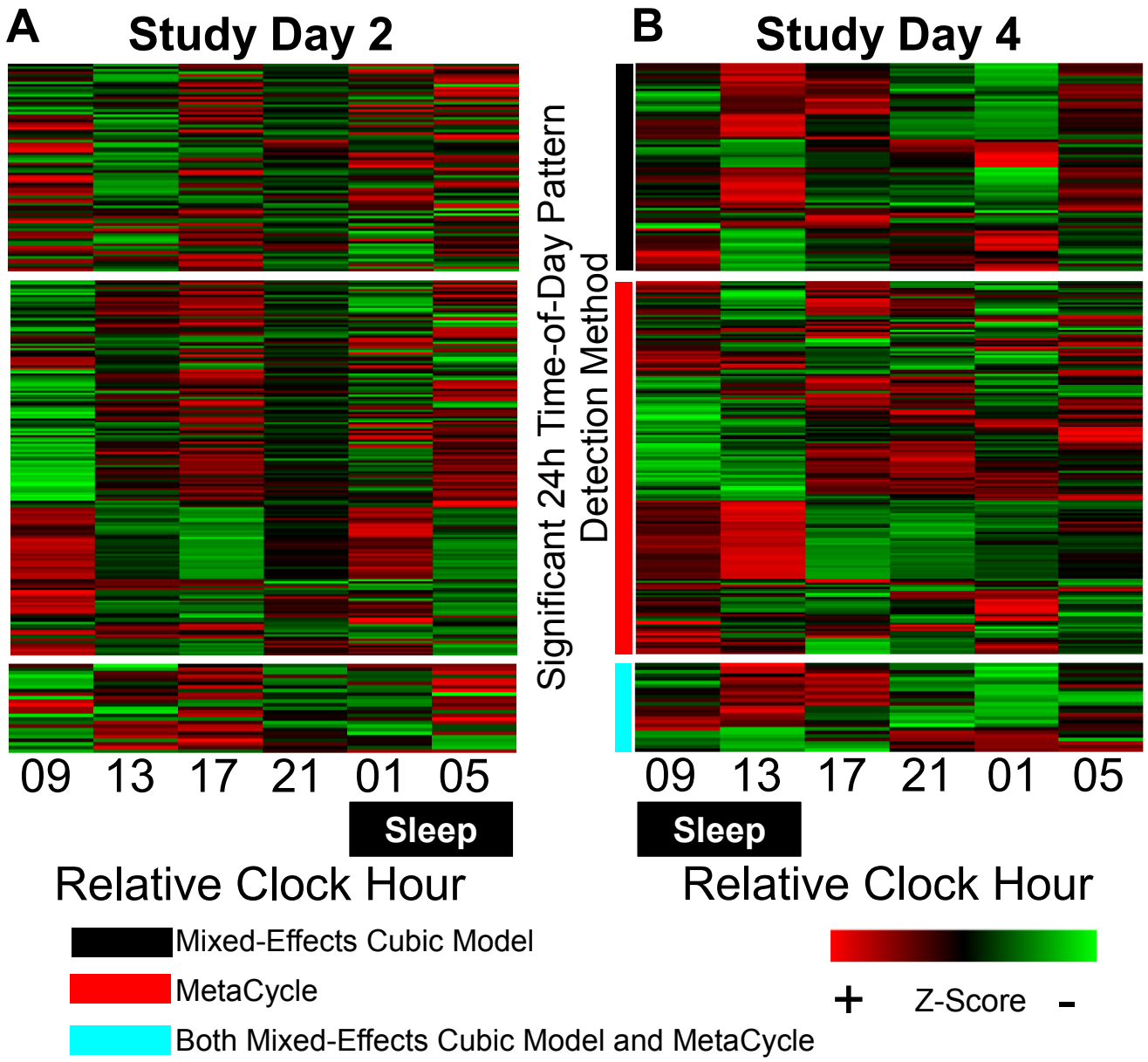

Figure S9. Heat-maps representing proteins with a significant 24h time-of-day pattern during circadian misalignment (study day 4). Average z-score profiles are represented for circadian alignment (A) and circadian misalignment (B). On the y axes, the black box indicates proteins with significant 24h time-of-day patterns detected by mixed-effects cubic models, the red box indicates proteins with significant 24h time-of-day patterns detected by MetaCycle, and the cyan box indicates proteins with significant 24h time-of-day patterns detected by both the mixed-effects cubic models and MetaCycle. Black boxes on the x axes represent the timing of scheduled sleep opportunities.

Additional data table S1 (separate file)

The table contains the full names and abbreviations for all proteins analyzed, the resulting *P*-values or False Discovery Rates (FDR) for the Significance Analysis of Microarray (SAM), linear mixed-effects cubic models, MetaCycle, Extraction of Differential Gene Expression (EDGE), and Detection of Differential Rhythmicity (DODR) analyses, the estimated phase differences between circadian alignment and misalignment for strongly circadian regulated proteins, indication of regulation by the circadian and behavioral cycles, and identification of protein cluster numbers corresponding to figure S1.

References

1. Olejnik S & Algina J (2003) Generalized eta and omega squared statistics: measures of effect size for some common research designs. *Psychol Methods* 8(4):434-447.
2. Bakeman R (2005) Recommended effect size statistics for repeated measures designs. *Behav Res Methods* 37(3):379-384.
3. Storey JD, Xiao W, Leek JT, Tompkins RG, & Davis RW (2005) Significance analysis of time course microarray experiments. *Proc Natl Acad Sci U S A* 102(36):12837-12842.
4. McHill AW*, et al.* (2014) Impact of circadian misalignment on energy metabolism during simulated nightshift work. *Proc Natl Acad Sci U S A* 111(48):17302-17307.
5. Morris CJ*, et al.* (2015) Endogenous circadian system and circadian misalignment impact glucose tolerance via separate mechanisms in humans. *Proc Natl Acad Sci U S A* 112(17):E2225-2234.
6. Kim MS & Lee DY (2015) Insulin-like growth factor (IGF)-I and IGF binding proteins axis in diabetes mellitus. *Ann Pediatr Endocrinol Metab* 20(2):69-73.
7. Rehman JU, Brismar K, Holmback U, Akerstedt T, & Axelsson J (2010) Sleeping during the day: effects on the 24-h patterns of IGF-binding protein 1, insulin, glucose, cortisol, and growth hormone. *Eur J Endocrinol* 163(3):383-390.
8. Lang CH, Vary TC, & Frost RA (2003) Acute in vivo elevation of insulin-like growth factor (IGF) binding protein-1 decreases plasma free IGF-I and muscle protein synthesis. *Endocrinology* 144(9):3922-3933.
9. Nam SY*, et al.* (1997) Effect of obesity on total and free insulin-like growth factor (IGF)-1, and their relationship to IGF-binding protein (BP)-1, IGFBP-2, IGFBP-3, insulin, and growth hormone. *Int J Obes Relat Metab Disord* 21(5):355-359.
10. Reyer A*, et al.* (2015) The RGD sequence present in IGFBP-2 is required for reduced glucose clearance after oral glucose administration in female transgenic mice. *Am J Physiol Endocrinol Metab* 309(4):E409-417.
11. Wheatcroft SB*, et al.* (2007) IGF-binding protein-2 protects against the development of obesity and insulin resistance. *Diabetes* 56(2):285-294.
12. Frystyk J, Skjaerbaek C, Vestbo E, Fisker S, & Orskov H (1999) Circulating levels of free insulin-like growth factors in obese subjects: the impact of type 2 diabetes. *Diabetes Metab Res Rev* 15(5):314-322.
13. Arafat AM*, et al.* (2009) The role of insulin-like growth factor (IGF) binding protein-2 in the insulin-mediated decrease in IGF-I bioactivity. *J Clin Endocrinol Metab* 94(12):5093-5101.
14. Hjortebjerg R*, et al.* (2017) The IGF system in patients with type 2 diabetes: associations with markers of cardiovascular target organ damage. *Eur J Endocrinol* 176(5):521-531.

15. Ning Y, *et al.* (2006) Diminished growth and enhanced glucose metabolism in triple knockout mice containing mutations of insulin-like growth factor binding protein-3, -4, and -5. *Mol Endocrinol* 20(9):2173-2186.
16. Jehle PM, Jehle DR, Mohan S, & Bohm BO (1998) Serum levels of insulin-like growth factor system components and relationship to bone metabolism in Type 1 and Type 2 diabetes mellitus patients. *J Endocrinol* 159(2):297-306.
17. Gleason CE, *et al.* (2010) Role of insulin-like growth factor-binding protein 5 (IGFBP5) in organismal and pancreatic beta-cell growth. *Mol Endocrinol* 24(1):178-192.
18. Liu Y, *et al.* (2015) Serum IGFBP7 levels associate with insulin resistance and the risk of metabolic syndrome in a Chinese population. *Sci Rep* 5:10227.
19. Lopez-Bermejo A, *et al.* (2006) Insulin resistance is associated with increased serum concentration of IGF-binding protein-related protein 1 (IGFBP-rP1/MAC25). *Diabetes* 55(8):2333-2339.
20. Law IK, *et al.* (2010) Lipocalin-2 deficiency attenuates insulin resistance associated with aging and obesity. *Diabetes* 59(4):872-882.
21. Heiker JT, *et al.* (2013) Vaspin inhibits kallikrein 7 by serpin mechanism. *Cell Mol Life Sci* 70(14):2569-2583.
22. Yamauchi T, *et al.* (2002) Adiponectin stimulates glucose utilization and fatty-acid oxidation by activating AMP-activated protein kinase. *Nature Med* 8(11):1288-1295.
23. Weyer C, *et al.* (2001) Hypoadiponectinemia in obesity and type 2 diabetes: close association with insulin resistance and hyperinsulinemia. *J Clin Endocrinol Metab* 86(5):1930-1935.
24. Crispim CA, *et al.* (2012) Adipokine levels are altered by shiftwork: a preliminary study. *Chronobiol Int* 29(5):587-594.
25. Zhang R, Lahens NF, Ballance HI, Hughes ME, & Hogenesch JB (2014) A circadian gene expression atlas in mammals: implications for biology and medicine. *Proc Natl Acad Sci U S A* 111(45):16219-16224.
26. Jelkmann W & Metzen E (1996) Erythropoietin in the control of red cell production. *Ann Anat* 178(5):391-403.
27. Chen LN, *et al.* (2015) Erythropoietin improves glucose metabolism and pancreatic beta-cell damage in experimental diabetic rats. *Mol Med Rep* 12(4):5391-5398.
28. Lim SK & Park SH (2011) High glucose stimulates the expression of erythropoietin in rat glomerular epithelial cells. *Lab Anim Res* 27(3):245-250.
29. Rajpathak SN, *et al.* (2009) The role of iron in type 2 diabetes in humans. *Biochim Biophys Acta* 1790(7):671-681.
30. Lee HJ, Choi JS, Kim WH, Park SI, & Song J (2015) Effect of excess iron on oxidative stress and gluconeogenesis through hepcidin during mitochondrial dysfunction. *J Nutr Biochem* 26(12):1414-1423.
31. Swaminathan S, Fonseca VA, Alam MG, & Shah SV (2007) The role of iron in diabetes and its complications. *Diabetes Care* 30(7):1926-1933.
32. Wang H, *et al.* (2014) Hepcidin is directly regulated by insulin and plays an important role in iron overload in streptozotocin-induced diabetic rats. *Diabetes* 63(5):1506-1518.
33. Vecchi C, *et al.* (2014) Gluconeogenic signals regulate iron homeostasis via hepcidin in mice. *Gastroenterology* 146(4):1060-1069.
34. Sasaki S, *et al.* (2014) Short sleep duration increases the risk of chronic kidney disease in shift workers. *J Occup Environ Med* 56(12):1243-1248.
35. Knutsson A (2003) Health disorders of shift workers. *Occup Med* 53(2):103-108.

36. Jorgensen JT, Karlsen S, Stayner L, Andersen J, & Andersen ZJ (2017) Shift work and overall and cause-specific mortality in the Danish nurse cohort. *Scand J Work Environ Health* 43(2):117-126.
37. Wu G, Anafi RC, Hughes ME, Kornacker K, & Hogenesch JB (2016) MetaCycle: an integrated R package to evaluate periodicity in large scale data. *Bioinformatics* 32(21):3351-3353.
38. Moller-Levet CS*, et al.* (2013) Effects of insufficient sleep on circadian rhythmicity and expression amplitude of the human blood transcriptome. *Proc Natl Acad Sci U S A* 110(12):E1132-1141.
39. Archer SN*, et al.* (2014) Mistimed sleep disrupts circadian regulation of the human transcriptome. *Proc Natl Acad Sci U S A* 111(6):E682-691.